A Self-Deleting AAV-CRISPR System
for *In Vivo* Genome Editing

Ang Li,[1] Ciaran M. Lee,[1] Ayrea E. Hurley,[2] Kelsey E. Jarrett,[2,3] Marco De Giorgi,[2] Weiqi Lu,[1] Karol S. Balderrama,[2] Alexandria M. Doerfler,[2] Harshavardhan Deshmukh,[1] Anirban Ray,[1] Gang Bao,[1] and William R. Lagor[2,3]

[1]Department of Bioengineering, Rice University, Houston, TX 77030, USA; [2]Department of Molecular Physiology and Biophysics, Baylor College of Medicine, Houston, TX 77030, USA; [3]Integrative Molecular and Biomedical Sciences Graduate Program, Baylor College of Medicine, Houston, TX 77030, USA

Adeno-associated viral (AAV) vectors packaging the CRISPR-Cas9 system (AAV-CRISPR) can efficiently modify disease-relevant genes in somatic tissues with high efficiency. AAV vectors are a preferred delivery vehicle for tissue-directed gene therapy because of their ability to achieve sustained expression from largely non-integrating episomal genomes. However, for genome editizng applications, permanent expression of non-human proteins such as the bacterially derived Cas9 nuclease is undesirable. Methods are needed to achieve efficient genome editing *in vivo*, with controlled transient expression of CRISPR-Cas9. Here, we report a self-deleting AAV-CRISPR system that introduces insertion and deletion mutations into AAV episomes. We demonstrate that this system dramatically reduces the level of *Staphylococcus aureus* Cas9 protein, often greater than 79%, while achieving high rates of on-target editing in the liver. Off-target mutagenesis was not observed for the self-deleting Cas9 guide RNA at any of the predicted potential off-target sites examined. This system is efficient and versatile, as demonstrated by robust knockdown of liver-expressed proteins *in vivo*. This self-deleting AAV-CRISPR system is an important proof of concept that will help enable translation of liver-directed genome editing in humans.

INTRODUCTION

Adeno-associated viral (AAV) vectors are a leading candidate for delivery of the CRISPR-Cas9 system to somatic tissues in humans. It has been shown that a CRISPR-Cas9 system packaged in AAV (AAV-CRISPR) can permanently modify disease-relevant genes in the liver,[1–4] retina,[5–8] brain,[9,10] heart,[11,12] and skeletal muscle.[13–15] However, as recombinant AAV genomes exist as stable episomes, there are regulatory and safety concerns arising from persistent expression of the bacterially derived Cas9 enzyme. Several systems that control Cas9 activity have been reported, including split-intein Cas9,[16,17] inducible promoters,[18] chemical control of protein stability,[19–21] and anti-CRISPR proteins.[22] While these methods can provide certain control of Cas9 activity, they cannot remove the Cas9 protein, and some of them require the use of additional non-human protein moieties.

The removal of a co-expressed transgene with CRISPR-Cas9 was first reported by Moore et al. in 2015,[23] where the *S. pyogenes* Cas9 was used to remove fluorescent reporters in cells. More recently, two systems, "KamiCas9"[24] and "Lenti-SLiCES"[25] used lentiviral vectors with a self-deleting guide RNA (gRNA) to eliminate Cas9 expression *in vivo*. However, the use of lentiviral vectors is not ideal for many gene therapy applications, due to the risks associated with random integration into the host genome. An AAV plasmid with Cas9 flanked by two gRNA target sites has been shown to mediate its own excision in HEK293FT cells[5]; however, *in vivo* testing of this system as an AAV vector has not been reported. Here, we report the development of a self-deleting AAV-CRISPR system using a CRISPR gRNA that cuts the Cas9 coding sequence *in vivo*, and we demonstrate that this system can effectively remove Cas9 protein in mouse liver while retaining efficient *in vivo* editing of endogenous targets without detectable off-target activity. This approach has the potential to circumvent problems associated with permanent Cas9 expression, enabling safe and efficient somatic genome editing in humans.

RESULTS

AAV-CRISPR Is Capable of Disrupting Episomal AAV Genomes *In Vivo*

The liver is one of the principal sites where AAV-based gene therapy is being applied successfully in humans. We tested whether AAV-CRISPR could disrupt a co-expressed AAV-GFP transgene in mouse liver. Fifteen possible GFP-targeting gRNAs (Table S1) were first screened in 293-GFP cells, and the most efficient one (Sa_G-13) was selected for *in vivo* studies (Figure S1). An AAV8 vector encoding *Staphylococcus aureus* Cas9 (SaCas9) and the GFP-targeting gRNA was co-delivered with an AAV expressing emerald GFP (EmGFP) in an equimolar ratio, and mouse livers were harvested 3, 7, 14, 21, and 28 days after delivery (Figure 1A). Cas9 cutting of the GFP transgene did not significantly reduce the genome copy number of AAV-GFP or AAV-SaCas9 episomes (Figures 1B and 1C). AAV-GFP editing rates increased in a linear fashion over time, reaching
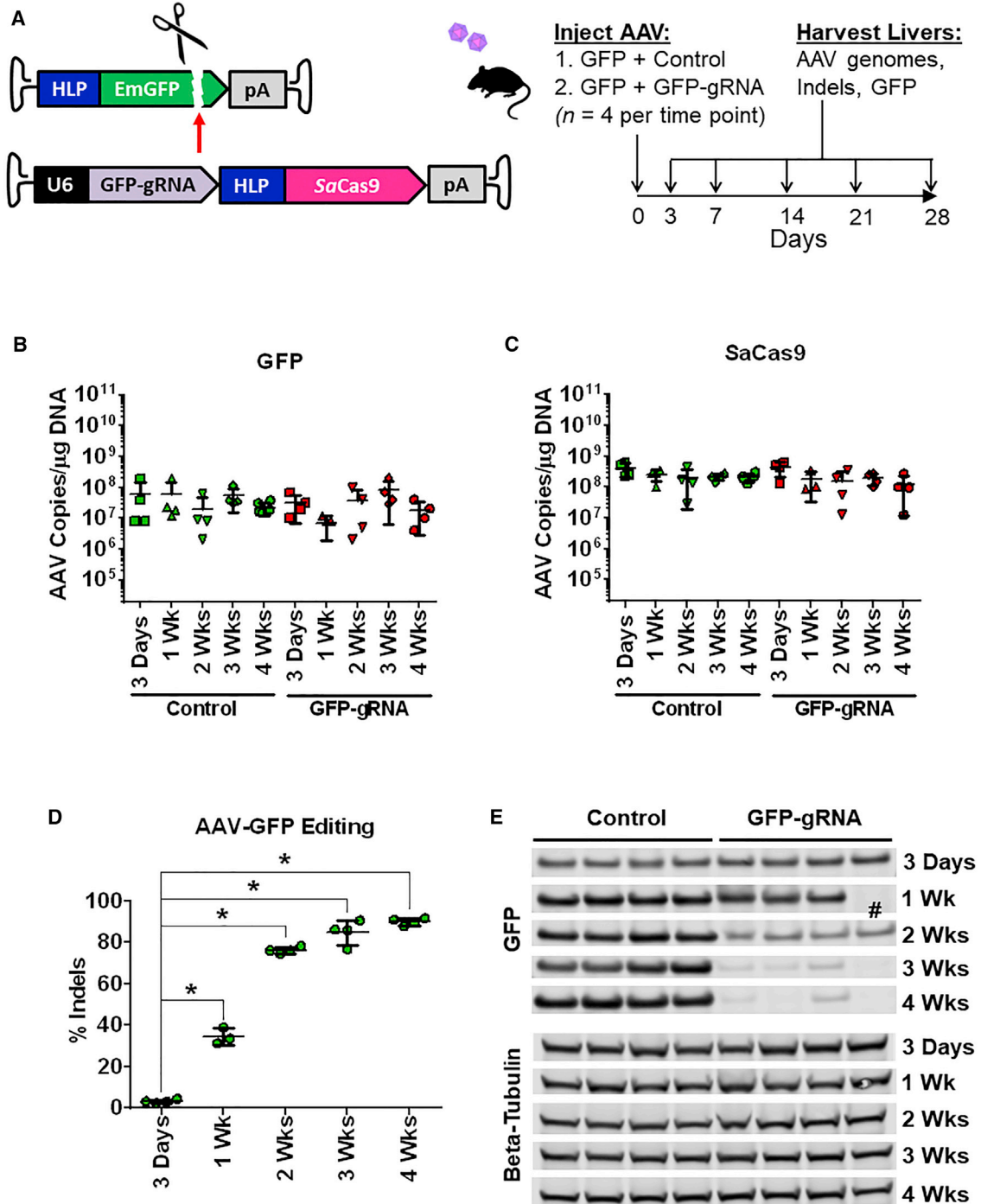
Figure 1. AAV-CRISPR Removal of an Episomal AAV Transgene

(A) AAV8 vectors encoding emerald GFP (EmGFP) under the control of a small liver-specific promoter, HLP (top), and SaCas9 driven by a synthetic liver-specific HLP promoter with either a control guide RNA (gRNA) or a GFP-targeted gRNA (bottom). Experimental timeline with treatment groups is shown at right. (B) AAV-GFP genome copy numbers. (C) AAV-SaCas9 genome copy numbers. (D) GFP indel rates calculated via next-generation sequencing (NGS). (E) Western blots for GFP and beta-tubulin in mouse livers treated with a control gRNA or GFP-gRNA vector. [#]Failed AAV injection based on the absence of detectable vector genomes by qPCR. Data are indicated as mean ± SD. *$p < 0.05$.

an average of 90% insertion or deletion (indel) rate after 4 weeks (Figure 1D). The GFP protein level was significantly reduced after 2 weeks and was virtually undetectable by 3 weeks (Figure 1E), establishing the proof of concept that CRISPR-Cas9 can eliminate AAV-expressed transgenes *in vivo*.

Screening the Activity of Self-Deleting gRNAs

To develop a self-deleting AAV-CRISPR platform, we first designed gRNAs targeting different functional domains of the SaCas9 coding sequence (Figure S2; Table S2). We then tested the activity of 19 potential self-deleting SaCas9 gRNAs *in vitro* using a firefly-luciferase-based single-strand annealing assay. Briefly, short oligos containing the gRNA target sites and corresponding protospacer-adjacent motif (PAM) were cloned between two direct repeats of a truncated firefly luciferase gene containing two intervening stop codons after the first repeat. Upon cutting by Cas9, the open fragments undergo recision, and the direct repeats anneal, forming a full-length functional firefly luciferase in a subset of DNA-repair events (Figure S3A). Firefly luciferase activity is proportional to cutting efficiency by CRISPR-Cas9, and the relative efficiencies of different gRNAs can be quantitatively measured.[26] The firefly luciferase reporter plasmids were co-transfected into HEK293FT cells along with a renilla luciferase control, SaCas9, and each candidate gRNA. The ratio of firefly:renilla luciferase activity of each self-deleting gRNA was normalized to that of the most efficient GFP-targeting gRNA. Seventeen of the 19 gRNA had detectable activity against SaCas9 target sites (Figure S3B). The "Self-5" gRNA had the highest activity, and was selected for further testing *in vivo* along with "Self-1," which disrupts the enzymatic RuvC-I nuclease domain closest to the start codon.

Testing Self-Deleting SaCas9 gRNAs *In Vivo*

We next sought to determine whether our self-deleting CRISPR system could reduce SaCas9 protein *in vivo*. To do this, we compared the Self-1 and Self-5 gRNAs for their ability to eliminate AAV-expressed SaCas9 protein in the liver. Male C57BL/6J mice were injected with an AAV-SaCas9 vector with a gRNA targeting an endogenous gene, either alone or in combination with a second AAV vector expressing either Self-1 or Self-5 (Figure S4A). SaCas9 protein was readily detectable by western blotting in livers at 1 month after injection. Interestingly, the protein levels of SaCas9 were similarly decreased by Self-1 and Self-5 relative to the mice receiving the SaCas9 vector alone (Figure S4B). Based on this, we selected Self-1 for further development, as indels near the N terminus would reduce the likelihood of creating immunogenic SaCas9 peptides. Additionally, Self-1 is located at the nuclease RuvC-like portion of SaCas9, which is potentially more critical to the activity of the nuclease than the REC domain, where Self-5 targets.

Dose-Response of SaCas9 Removal with the Self-1 gRNA

We next tested whether increasing the molar ratio of Self-1 to SaCas9 vector would more efficiently remove SaCas9 protein. Male C57BL/6J mice were injected with an AAV vector encoding SaCas9 and a gRNA targeting an endogenous gene (*Mttp*). A second AAV vector expressing the self-deleting gRNA (Self-1) was co-delivered at a 1:1, 1:2, or 1:3 molar ratio (Figure 2A). To ensure that editing could reach its maximal value, these animals were followed for 6 weeks prior to liver harvest. Self-deletion of SaCas9 did not significantly reduce AAV genome copy number, as seen previously with AAV-GFP (Figures 2B and 2C). Without the self-deleting gRNA, indels at the endogenous target site (*Mttp*) were present at a frequency of 28% via next-generation sequencing (NGS). With the self-deleting gRNA co-delivered, the indel rates at the endogenous *Mttp* target site were significantly lower, at 15%, 9%, and 7%, respectively, with increasing Self-1 doses (Figure 2D). The 1:3 ratio of Cas9:Self-1 resulted in slightly lower endogenous editing efficiency, as compared to a 1:1 ratio (7% versus 15%; $p < 0.05$). Disruption of the SaCas9 transgene ranged from 18% to 23% via Tracking of Indels by Decomposition (TIDE), with minimal variation between the self-deleting groups (Figure 2E). SaCas9 protein level in liver tissue was significantly reduced in all three groups receiving the self-deleting gRNA vector (down 70%, 84%, and 84%) (Figures 2F and 2G) but with no significant differences among the three ratios tested.

Endogenous and Self-Deleting SaCas9 gRNAs Exhibit No Measurable Off-Target Activity

A critical concern regarding current CRISPR-Cas9-based gene editing strategies is the cutting activity at potential off-target sites. These off-target events may cause unwanted tumorigenic mutations or large chromosomal rearrangements. Potential off-target sites were first identified *in silico* using the bioinformatics tool COSMID[27] and subsequently examined using targeted NGS. Of the 8 potential off-target sites associated with the *Mttp*-targeting gRNA, only off-target site 3 (OT3) showed indel formation above background levels at a low rate of 0.13%–0.22% (Figure 3A). However, on closer inspection of the reads, this site occupies an area of five direct Gs and most likely represents PCR and sequencing error due to the chemistry of the Illumina platform. The self-deleting gRNA at the highest dose did not display any detectable off-target cutting activity at the 22 predicted potential off-target sites (Figure 3B). NGS revealed 38% indel rates at the SaCas9 locus at the highest self-deleting gRNA dose, indicating a robust on-target cutting activity.

Timing of AAV-CRISPR Self-Deletion

We next examined the time course of SaCas9 self-deletion in relation to an endogenous target. Mice were injected with an AAV-SaCas9 vector targeting *Mttp* alone or in combination with a 1:1 molar ratio of Self-1. Livers were harvested at 1, 2, and 4 weeks from the mice receiving Self-1 and compared to those from animals with SaCas9 alone at 4 weeks (Figure S5A). *Mttp* and SaCas9 self-editing rates increased in a linear fashion between 1 and 4 weeks (Figures S5B and S5C). At the protein level, SaCas9 was lower at all time points with the self-deleting gRNA (Figure S5D). The lower level of SaCas9 protein at 1 and 2 weeks is likely a result of the normal gradual increase in AAV expression in this tissue (which typically requires 10–14 days to reach its peak) rather than self-deletion. Since self-deletion occurs simultaneously with on-target cutting, we reasoned that higher rates of on-target editing might be achieved by slightly delaying the delivery of Self-1. To test this,
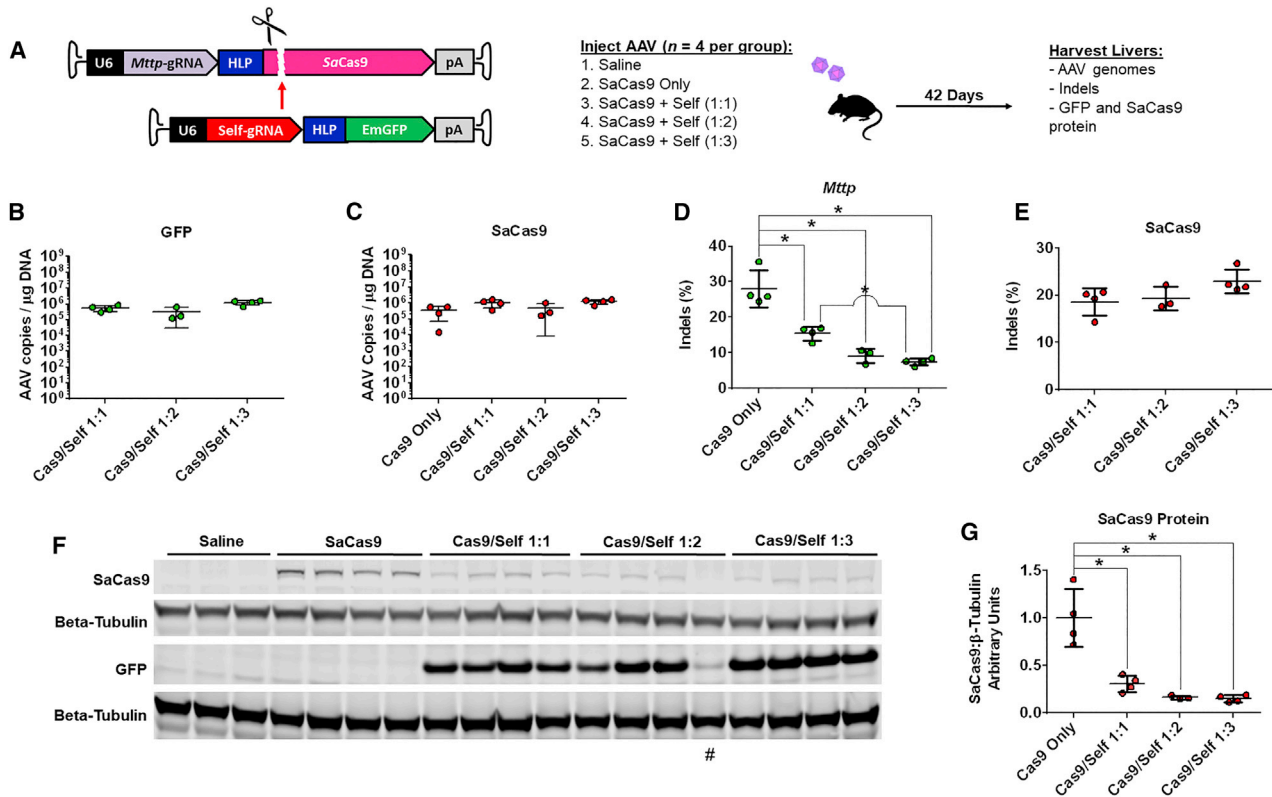
**Figure 2. AAV-CRISPR-Mediated Removal of SaCas9 *In Vivo***

(A) An AAV8 vector expressing a gRNA targeting mouse *Mttp* and SaCas9 was co-injected with a separate AAV8 vector expressing a self-deleting gRNA and GFP. Experimental design and timeline are shown on the right. (B and C) EmGFP (B) and SaCas9 (C) genome copies were analyzed via qPCR between treatment groups. (D) *Mttp* editing rates by NGS. (E) SaCas9 editing rates by TIDE. (F) Western blots for SaCas9 (against a hemagglutinin [HA] tag) and GFP between in all treatment groups. (G) Densitometry of SaCas9 relative to β-tubulin. #Failed AAV injection based on the absence of detectable vector genomes by qPCR. This data point was removed from all panels for clarity, with the exception of the western blot. Data are indicated as mean ± SD. *p < 0.05.

we compared mice injected with SaCas9 targeting *Mttp* alone, mice that received a co-injection of Self-1, and a third group that received the injection of Self-1 5 days later (Figure S6A). Robust editing of the endogenous target was observed with 24% for AAV-SaCas9 alone. In this experiment, on-target editing decreased dramatically with co-injection of Self-1. Interestingly, endogenous editing was preserved in the group receiving Self-1 after the 5-day delay (26%) (Figure S6B). However, this group had no detectable self-deletion and a complete absence of GFP protein, indicating that Self-1 did not transduce the liver in these mice (Figures S6C and S6D). Thus, it appears that even as early as 5 days after AAV8 administration, additional AAV8 vectors are blocked from entering the murine liver by the host immune system.

Versatility for Editing Different Genomic Targets

We next sought to determine whether our self-deleting gRNA system could achieve comparable editing efficiency at other endogenous targets. To test this, we selected the low-density lipoprotein receptor (*Ldlr*) and the apolipoprotein E (*Apoe*) genes. LDLR and ApoE are primarily liver-expressed proteins involved in the clearance of

ApoB-containing lipoprotein particles, and both are potential targets for therapeutic genome editing. Mice were injected with SaCas9 vectors with gRNAs targeting either *Ldlr* or *Apoe*, with or without co-injection of Self-1 at a 1:1 ratio, and followed for 28 days (Figure 4A). High levels of on-target editing were observed for both *Ldlr* and *Apoe*, and this was not significantly reduced with co-injection of Self-1 (*Ldlr*: 41.9% versus 37.5%; *Apoe*: 33.8% versus 30.4%) (Figures 4B and 4C). Co-injection of Self-1 introduced indels in the AAV-SaCas9 vector targeting *Ldlr* (25.9%) as well as *Apoe* (50.1%) at high frequency (Figure 4D). In the liver, LDLR protein was decreased by 80% with AAV-SaCas9 alone, and a similar 79% reduction was achieved with the addition of Self-1 (Figures 4E and 4F). Although SaCas9 protein was not completely eliminated by Self-1, it was decreased by 73%, relative to AAV-SaCas9 alone (Figure 4G). Likewise, ApoE protein was reduced in plasma from mice treated with or without Self-1 (70% versus 62%), indicating highly efficient disruption of this primarily liver-expressed secreted protein (Figures 4H and 4I). SaCas9 protein levels dropped by 79% with Self-1 co-injection, showing a second example with efficient on-target editing despite SaCas9 self-deletion (Figure 4J).

A Mttp Indels

B SaCas9 Indels
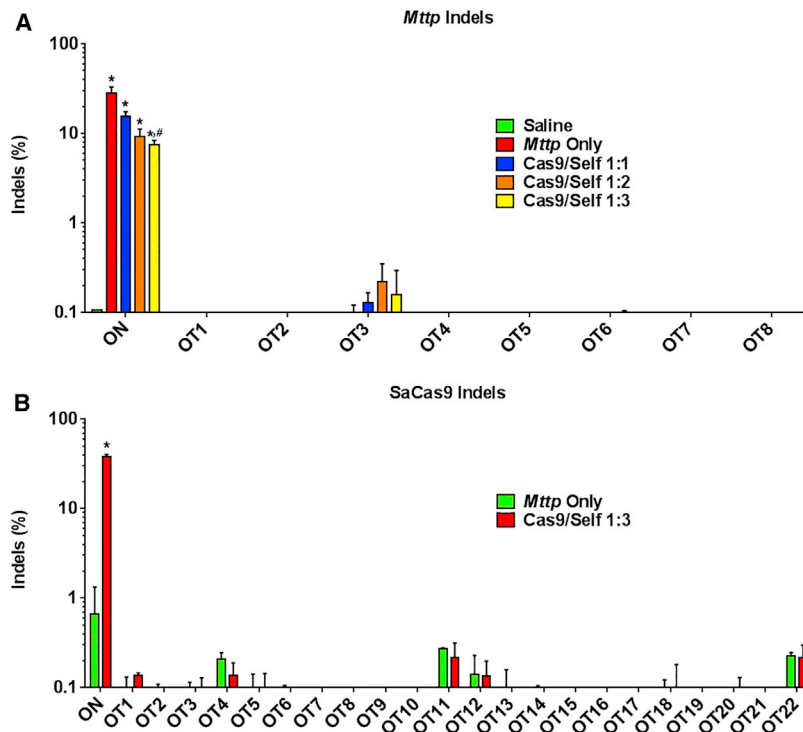
Figure 3. Endogenous *Mttp* and SaCas9 gRNAs Exhibit No Detectable Off-Target Activity

(A) NGS revealed no detectable off-target activity at 8 potential sites of the *Mttp* gRNA. The asterisk (*) indicates significance against saline-injected group, and the pound symbol (#) indicates significance against Self/Cas9 1:1 via one-way ANOVA and Tukey's post hoc multi-comparisons test. (B) Self-deleting gRNA revealed no detectable off-target activity *in vivo* at the highest dose of gRNA (1:3). OT1's higher indel rate is due to direct "G" repeats in the sequence. Data are indicated as mean ± SD. *$p < 0.05$.

both forward and reverse orientations (Figures 6B–6E). The nonspecific bands in mice treated with the SaCas9 vectors alone likely arise from self-priming of AAV episomes and their concatamers. Collectively, these data highlight an important pitfall to the use of AAV vectors for CRISPR-Cas9-based genome editing due to unwanted AAV vector insertions at genomic target sites.

DISCUSSION

Here, we report a self-deleting AAV-CRISPR system and demonstrate its utility in gene editing of the liver, one of the principal tissues currently being targeted with AAV gene therapy in humans. We show that a self-deleting gRNA targeting the coding sequence of SaCas9 can introduce inactivating mutations in AAV episomes *in vivo*. This results in efficient, although not complete, elimination of the SaCas9 protein over several weeks. For most targets, SaCas9 can be dramatically reduced without significantly compromising on-target editing. Off-target mutagenesis was not detected with the self-deleting gRNA or with the on-target gRNA at predicted sites in the mouse genome, consistent with the reported high specificity of SaCas9.[34] Importantly, we also uncover an unexpected safety concern due to the insertion of whole and truncated AAV vector genomes at endogenous loci cut with AAV-CRISPR.

AAV-CRISPR has been used in recent years to modify endogenous genes in the liver, heart, skeletal muscle, retina, and brain. However, to our knowledge, this is the first demonstration that AAV-CRISPR can disrupt recombinant AAV episomes with high efficiency *in vivo*. In designing this approach, we intended to cut AAV episomes with Cas9 to promote their degradation. Interestingly, this did not occur for either AAV-GFP or AAV-SaCas9 and suggests that the liver favors non-homologous end joining (NHEJ) repair of blunt-ended extrachromosomal DNA over degradation. Despite this, inactivating mutations introduced into AAV episomes can efficiently silence transgene expression. In the case of our self-deleting SaCas9 system, the levels of this nuclease are reduced 79% or more at the protein level. For some targets (*Ldlr* and *Apoe*), efficient endogenous editing and knockdown of the protein was achieved with SaCas9 self-deletion, although a decrease

Self-Deletion Generates Novel AAV Integration Patterns

Recombinant AAV are believed to be largely non-integrating in the absence of *Rep*,[28] and integration events in human gene therapy studies appear to be rare and randomly distributed.[29,30] However, we and others have previously reported insertion of fragments of inverted terminal repeats (ITRs) from AAV vectors at CRISPR-Cas9-generated double-strand breaks,[2,3] as well as whole vector genome insertions.[31–33] We next performed an experiment to check for possible vector insertions with our self-deleting system. Specifically, we performed PCR using primers flanking both sides of the cut site at each of the genomic loci (*Mttp*, *Ldlr*, and *Apoe*). An additional primer that binds to GFP in the Self-1 vector was used in combination with these to survey for whole genome insertions (Figure 5A). For all primer sets, no amplification was observed with DNA from mice injected with saline or with the SaCas9 vector alone. Amplicons consistent with whole vector genome integrations of the Self-1 vector were found in both forward and reverse orientations at all target sites (Figures 5B–5E). Products of the correct predicted size, including the ITR region, were observed in almost all samples. There was no clear relationship between time or dose and the degree of AAV genome insertion (Figures 5B and 5C). Truncated fragments of the SaCas9 vector could also participate in homology-independent targeted integration (HITI) as a result of self-cutting, where the breakpoint in the AAV-SaCas9 vector could directly fuse with the break at the genomic site. Primers were designed to detect integration of truncated AAV-SaCas9 vector genomes at each side of the endogenous target sites (Figure 6A). PCR confirmed novel HITI insertion patterns of Cas9-truncated AAV genomes in
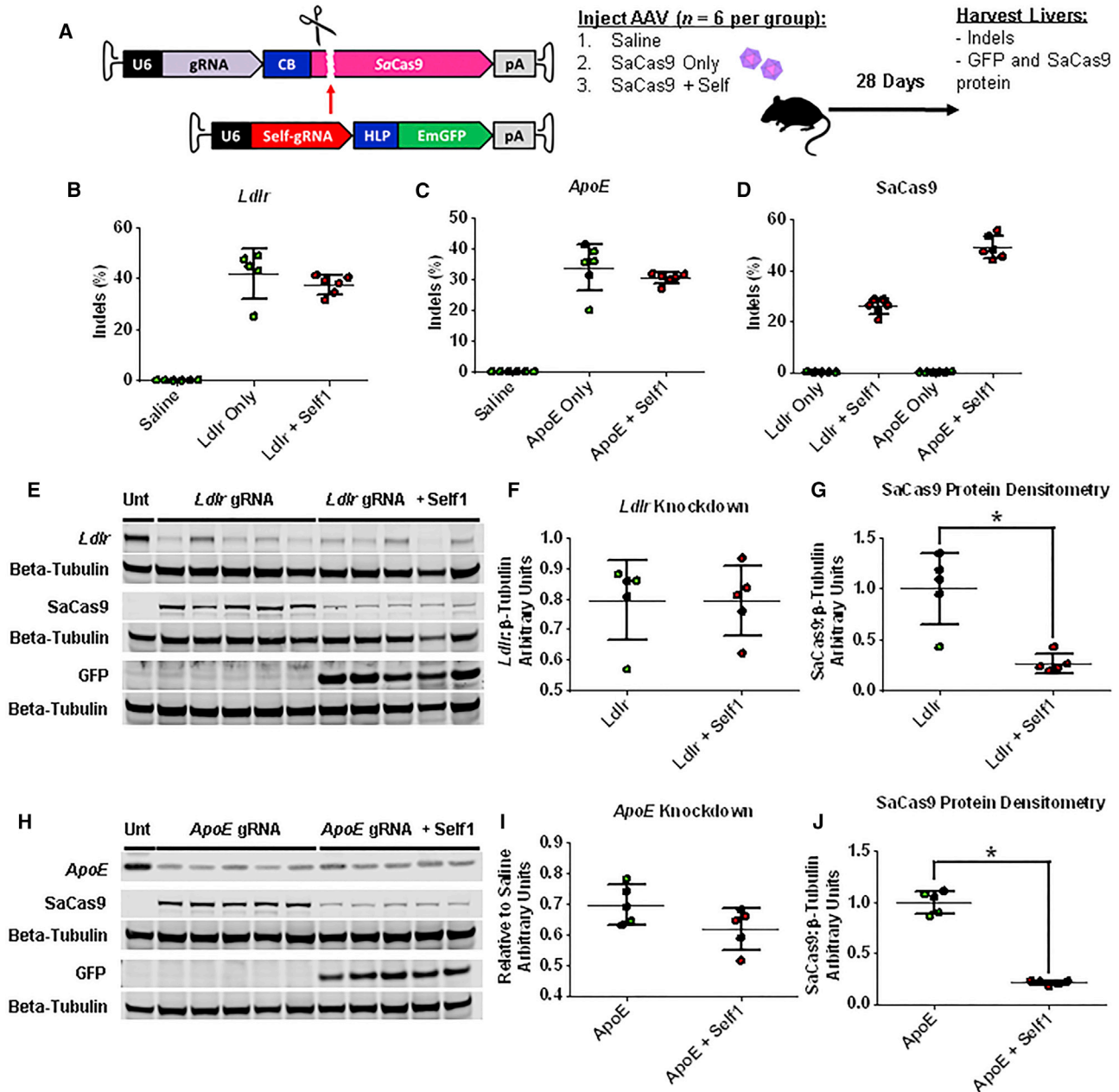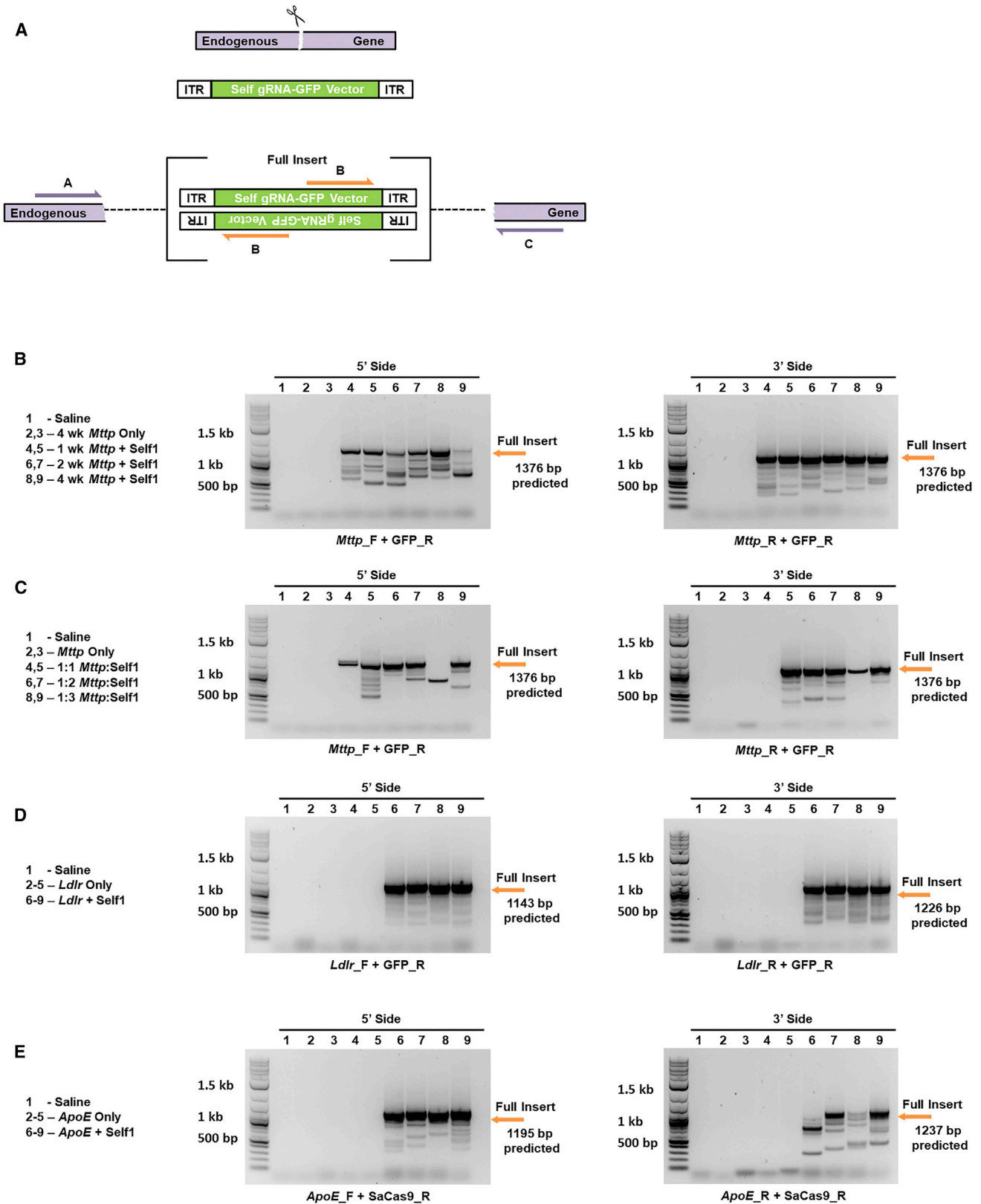
Figure 4. Robust Simultaneous Editing of Two Endogenous Targets with Self-inactivating AAV-CRISPR

(A) An AAV8 vector expressing a gRNA targeting either mouse low-density lipoprotein receptor (*Ldlr*) or apolipoprotein E (*Apoe*) was co-injected with a separate AAV8 vector expressing a self-deleting gRNA and GFP. Experimental design and timeline are shown on the right. (B) *Ldlr* editing rates by NGS. (C) *ApoE* editing rates by NGS. (D) SaCas9 editing rates by NGS. (E) Western blots for *Ldlr*, SaCas9 (against an HA tag), and GFP between treatment groups. Unt, untreated. (F) Densitometry of *Ldlr* to β-tubulin showing loss against the saline-treated group. (G) Densitometry of SaCas9 relative to β-tubulin. (H) Western blots for *Apoe*, SaCas9 (against an HA tag), and GFP between treatment groups. (I) Densitometry of *Apoe* showing loss relative to the saline-treated group. (J) Densitometry of SaCas9 relative to β-tubulin. Data are indicated as mean ± SD. *$p < 0.05$.

in on-target efficiency was seen for *Mttp*. The relative molar excess of AAV episomes within the cell may serve as a natural delay switch, allowing for the editing of endogenous targets before a complete dropoff in SaCas9 activity occurs.

Our self-deleting AAV-CRISPR system relies on efficient co-transduction with two different AAV vectors, and variations in co-delivery may explain some differences in editing efficiency for *Mttp* versus *Ldlr* and *Apoe*. Ideally, a single vector system would be preferred,

A

B

1 - Saline
2,3 – 4 wk *Mttp* Only
4,5 – 1 wk *Mttp* + Self1
6,7 – 2 wk *Mttp* + Self1
8,9 – 4 wk *Mttp* + Self1

5' Side — *Mttp*_F + GFP_R — Full Insert 1376 bp predicted

3' Side — *Mttp*_R + GFP_R — Full Insert 1376 bp predicted

C

1 - Saline
2,3 – *Mttp* Only
4,5 – 1:1 *Mttp*:Self1
6,7 – 1:2 *Mttp*:Self1
8,9 – 1:3 *Mttp*:Self1

5' Side — *Mttp*_F + GFP_R — Full Insert 1376 bp predicted

3' Side — *Mttp*_R + GFP_R — Full Insert 1376 bp predicted

D

1 - Saline
2-5 – *Ldlr* Only
6-9 – *Ldlr* + Self1

5' Side — *Ldlr*_F + GFP_R — Full Insert 1143 bp predicted

3' Side — *Ldlr*_R + GFP_R — Full Insert 1226 bp predicted

E

1 - Saline
2-5 – *ApoE* Only
6-9 – *ApoE* + Self1

5' Side — *ApoE*_F + SaCas9_R — Full Insert 1195 bp predicted

3' Side — *ApoE*_R + SaCas9_R — Full Insert 1237 bp predicted

(legend on next page)

which would guarantee simultaneous delivery of on-target and self-deleting gRNA to the same cells. Our attempts to develop a single vector system in which the self-deleting gRNA was co-expressed in *cis* with SaCas9 were unsuccessful. Even with the use of liver-specific promoters, indel mutations were introduced into the AAV genomes during viral packaging and did not express SaCas9 *in vivo* (data not shown). In addition, accommodating an on-target gRNA in the same vector would be a significant engineering challenge, due to the packaging limits of AAV vectors. However, given that we have established proof of concept for AAV-SaCas9 self-removal, and recent successes in AAV gene therapy in humans, this merits further exploration.

Our self-deleting AAV-CRISPR system generally reduces SaCas9 protein in the range of 70% to 84%. It is interesting to note that there is always residual SaCas9 in the liver with this approach, even at 4–6 weeks after AAV administration. One possible explanation is that there is imperfect overlap in the hepatocytes transduced with AAV-SaCas9 and Self-1. In our experience, the doses we used will deliver to 98%–99% of hepatocytes, and very efficient removal of LDLR and ApoE protein were achieved. Therefore, this probably does not solely account for the residual SaCas9 protein. A second possibility is that there may be a negative-feedback loop present. Since the enzymatic activity of SaCas9 is critical for its own disruption, the system could reach a steady state corresponding to a theoretical minimum, below which the remaining SaCas9 protein cannot effectively edit the AAV episomes encoding it. While it would be ideal to completely remove SaCas9 protein for clinical applications, this may not be feasible or absolutely essential. Rather, substantial decreases in SaCas9 protein may be acceptable in the liver, which is a highly regenerative tissue. Even if a handful of SaCas9-positive cells persist, these might be eliminated by the host immune system without significant pathological consequences, in much the same way as AAV capsid-presenting hepatocytes are purged by cytotoxic T cells.[35] Since genome editing is a permanent modification, durable therapeutic benefit could still be achieved, provided most of the edited hepatocytes either survive or expand to repopulate the liver.

The integration of full as well as truncated AAV genomes at CRISPR-Cas9-generated cut sites is a novel and unexpected finding. The risk of insertional mutagenesis is an important safety concern for any gene therapy, which certainly has significant implications for the clinical use of AAV-based genome editing. It is well known that treatment of neonatal mice with high doses of recombinant AAV vectors can result in tumor formation in the liver through integration into the *Rian* locus, via *cis*-acting effects of strong promoter elements.[36] Likewise, a recent report identified wild-type AAV2 integrations in known tumor suppressors and proto-oncogenes in human hepatocellular carcinoma biopsies.[37] While the relevance of these findings to humans receiving recombinant AAV gene therapy is a subject of debate,[38] it is clear that insertional mutagenesis should be avoided as much as possible. In the context of delivery of CRISPR-Cas9 with AAV vectors, insertion of whole vector genomes could be particularly problematic, as this event creates an artificial "hot spot" for integration, which will occur far more frequently than other homology-driven events. The risk of tumorigenesis with whole vector genome insertions is unknown but would likely depend on the transgene promoter activity, the gene being edited, and the genomic context of the target site.

Immunity to Cas9 has been found in humans[39] (https://www.biorxiv.org/content/biorxiv/early/2018/01/05/243345.full.pdf), and mice,[40] and there is concern that prolonged Cas9 expression could provoke elimination of edited cells and severe tissue damage. Our self-deleting system would significantly limit the window of SaCas9 protein expression in the majority of hepatocytes, though not completely eliminating it from all cells. Although cytotoxic T cells respond to AAV capsids in humans receiving liver-directed gene therapy with AAV, this can be effectively managed with prednisone.[41] Short-term immunosuppression is now becoming standard practice for AAV trials in humans, and it is believed that prednisone preserves transgene expression by delaying T cell responses until AAV capsids are cleared. The risks of genome editing with CRISPR-Cas9 in human liver are currently unknown, but these could likely also be mitigated by immunosuppression prior to Cas9 elimination. Our self-deleting AAV-CRISPR system establishes critical proof of concept that transient expression of Cas9 with AAV vectors can be achieved, capitalizing on the unparalleled delivery efficiency of this vector system. Refinements to the current self-deleting AAV-CRISPR system are needed to provide complete Cas9 removal while avoiding insertional mutagenesis at CRISPR-Cas9 on-target cut sites.

MATERIALS AND METHODS
gRNA Design
gRNAs were designed targeting *S. aureus* Cas9, GFP, *Mttp* (exon 2), and *Apoe* (exon 2) by manual inspection based on the presence of a canonical NNGRRT PAM at the target site. Potential off-target sites were identified using the web-based bioinformatics program CRISPR Off-target Sites with Mismatches, Insertions and/or Deletions (COSMID).[27] Search criteria for off-target sites included an NNGRR PAM (instead of NNGRRT), and a maximum of 3 mismatches and 2 base insertions or deletions relative to the target in the *M. musculus* (Mm10 build) genome. gRNAs with closely matching off-target sites were excluded and redesigned. gRNA sequences are shown in Table S2.

Figure 5. AAV Whole Genome Insertions at a CRISPR-Generated Cut Site

(A) Primers were designed to detect full-length AAV vector genome integrations from the 5′ and 3′ sides of the cut site. The endogenous gene-specific primers A and C are unique to the *Mttp*, *Ldlr*, and *Apoe* loci, while the AAV genome primer B is common. (B) AAV-Self-1 genome insertions in the *Mttp* locus are present in both forward and reverse orientations and do not increase from 1–4 weeks. (C) AAV-Self-1 insertions at the *Mttp* locus are not affected by increasing Self-1 dose. (D) AAV-Self-1 insertions in both orientations in the *Ldlr* locus. (E) AAV-Self-1 insertions in both orientations in the *Apoe* locus.
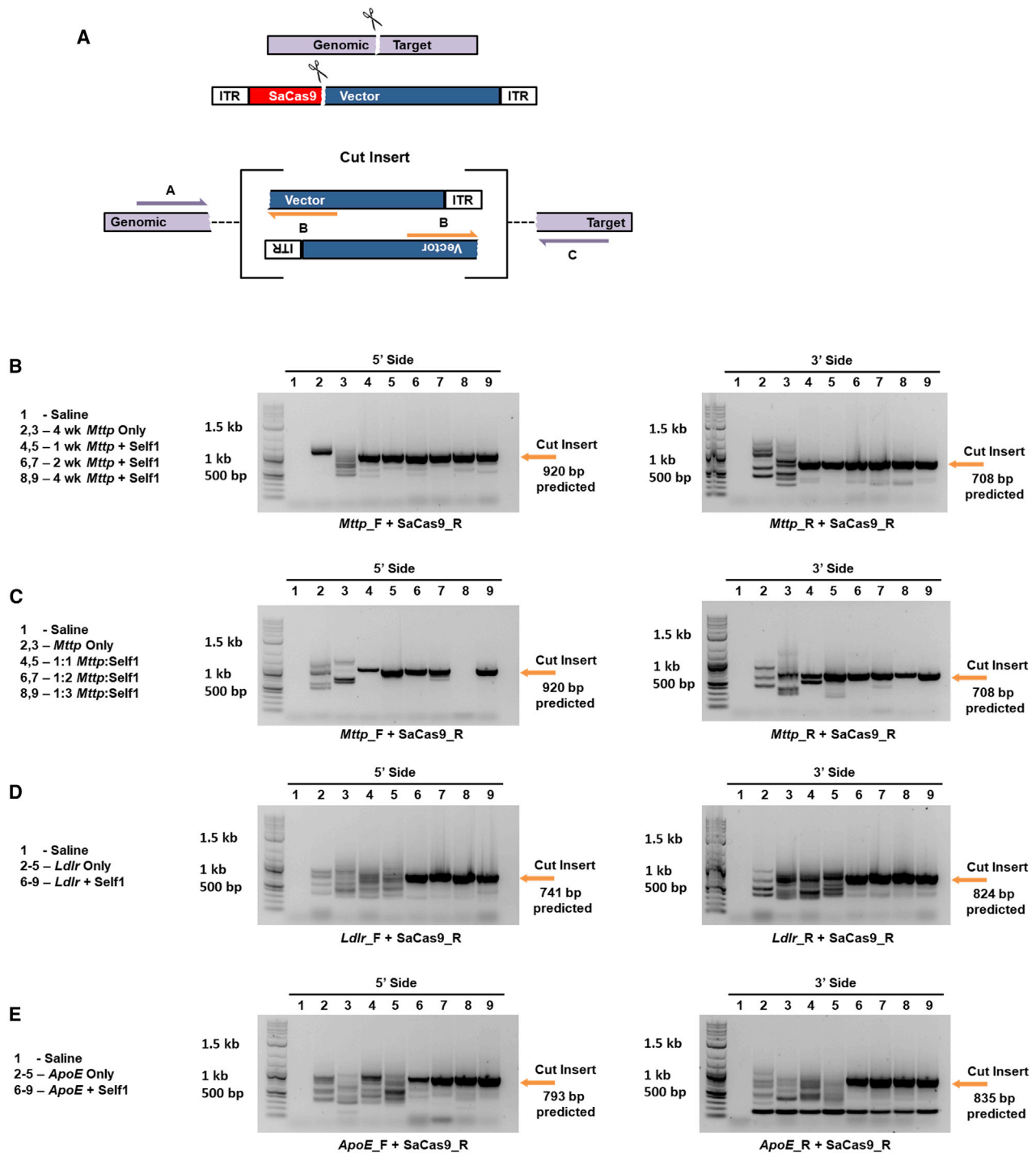
Figure 6. HITI Insertions of Truncated AAV-SaCas9 Vector Genomes at Endogenous Target Sites

(A) Partial AAV genomes are capable of integrating into endogenous gene targets after self-editing via homology-independent targeted integration (HITI). Primers were designed to detect self-edited vector integration from the 5′ and 3′ side of the target site. Primers A and C are specific to the target locus, while primer B is common within AAV-SaCas9 near the breakpoint. (B) Truncated AAV genome insertions with self-editing detected at the *Mttp* locus at 1–4 weeks after AAV. (C) Dosage of self-deleting gRNA does not change the frequency of truncated AAV vector insertion at the *Mttp* locus. (D) Truncated AAV genome insertions at the *Ldlr* locus with self-editing. (E) Truncated AAV genome insertions at the *Apoe* locus with self-editing. For all targets, nonspecific bands in lanes without Self-1 likely arise from aberrant priming of AAV-SaCas9 episomal DNA and concatamers.

Plasmid Construction

Luciferase SaCas9 targets were cloned into the pLV45.1-SSA-Luciferase backbone. AAV plasmids containing the ITRs from AAV2 were used to construct CRISPR plasmids using gene synthesis and standard molecular biology approaches. Plasmid 1162_pAAV-HLP-EmGFP-spA encodes Emerald GFP driven by a small synthetic liver-specific promoter, HLP.[42] Plasmid 1313_pAAV-U6-BbsI-MluI-gRNA-SA-HLP-SACas9-HA-OLLAS-spA encodes the SaCas9 transgene derived from px602 (Addgene plasmid #61593, a gift from Feng Zhang)[1] for liver-specific expression, with an upstream gRNA cloning cassette. gRNAs targeting GFP or *Mttp* were constructed using the plasmid 1313 backbone, yielding 1518_pAAV-U6-SA-eGFP-gRNA-HLP-SACas9-HA-OLLAS-spA and 1476_ pAAV-U6-Mttp-gRNA-SA-HLP-SACas9, respectively. A self-deleting gRNA targeting the RuvC domain of the *S. aureus* Cas9 gene was separately cloned into a similar backbone upstream of EmGFP (1530_pAAV-U6-BbsI-gRNA-SA-HLP-EmGFP), generating 1531_pAAV-U6-Self1-gRNA-SA-HLP-EmGFP. Targeting of *Ldlr* was accomplished using the previously described 1375_pAAV8-U6-SA-WTmLdlrEx14-gRNA2-N22-CB-SACas9-HA-OLLAS-spA vector.[31] A gRNA targeting *Apoe* was cloned into 1255_pAAV-U6-SA-BbsI-MluI-gRNA-CB-SACas9-HA-OLLAS-sPa,[31] generating 1377_pAAV8-U6-SA-mApoE-Exon2-gRNA2-N22-CBSACas9-HA-OLLAS-spA. All clones were verified by sequencing, as well as individual digestion with XmaI, SnaBI, and PvuII to confirm intact ITRs. Complete sequences are listed in the Supplemental Information, and plasmids are publicly available on Addgene or upon request.

Single-Strand Annealing Assay for gRNA Screening

24 hr prior to transfection, 10,000 HEK293FT cells were seeded into 96-well plates. Transfections were performed in triplicate, with each mix containing 100 ng DNA measured by Qubit and 0.4 μL Lipofectamine 2000. A typical reaction contained 20 ng Firefly target, 40 ng px601 (Addgene plasmid #61591, a gift from Feng Zhang), 24 ng self-editing plasmid, 4 ng renilla, and 11 ng pUC19 plasmid. Luciferase expression was measured 48 hr post-transfection using the Dual-Glo Luciferase Assay System (Promega, E2920).

AAV Production

AAVs were generated as previously described,[3,43] with several modifications. The adenoviral helper plasmid pAdDeltaF6 (PL-F-PVADF6) and AAV packaging plasmid pAAV2/8 (PL-T-PV0007) were obtained from the University of Pennsylvania Vector Core. These plasmids were co-transfected with the AAV transgene construct into 293T cells using polyethylenimine (PEI). Cell pellets were harvested and purified using a single CsCl density gradient centrifugation. Fractions containing AAV vector genomes were pooled and then dialyzed in 100,000 molecular weight cut off (MWCO) cassettes against three washes of PBS at 4°C overnight to remove CsCl. Purified AAVs were then concentrated using an Amicon 100-kDa MWCO centrifugal filtration device (UFC510024) before storage at −80°C until use. AAV titers were calculated after DNase digestion using qPCR against a standard curve and primers specific to *S. aureus* Cas9 and GFP (Table S5).

Animals

Male C57BL/6J mice, 6–8 weeks of age, were obtained from Jackson Laboratories and kept with a light cycle from 7 a.m. to 9 p.m. Animals were allowed free access to food and water and maintained on a standard chow diet. Individual AAV vectors were injected at a dose of 5×10^{11} genome copies (GCs) per animal, with exception of the self-deleting vector, which ranged from 5×10^{11} to 1.5×10^{12} GCs per mouse. AAVs were diluted in 300 μL sterile PBS and delivered via intraperitoneal injection. All treatment conditions were randomly allocated within each cage of mice at the time of injection. Mice were fasted 5 hr prior to injection and all subsequent blood collection. Blood was collected via retro-orbital bleeding using heparinized Natelson collection tubes, and plasma was isolated by centrifugation at $10,000 \times g$ for 20 min at 4°C. All experiments were approved by the Baylor College of Medicine Institutional Animal Care and Use Committee (IACUC) and performed in accordance with institutional guidelines under protocol numbers AN-6243 and AN-7243.

TIDE Analysis

Primers amplifying the target regions were designed flanking the cut site, approximately 350 bp away on each side (Table S2). The gene of interest was then amplified via PCR, and the products were separated with electrophoresis on agarose gels and extracted using the QIAquick Gel Extraction Kit (QIAGEN, catalog no. 28704). Primers designed for PCR amplification were then used for Sanger sequencing of the targeted regions. Indel percentages were calculated via TIDE,[44] using a control chromatogram for comparison. Decomposition windows, left boundaries, and indel ranges were optimized to have the highest alignment possible. The significance cutoff was maintained at p < 0.001 for all analyses. Primers are provided in Table S3.

Western Blotting

Liver lysates were prepared by homogenizing liver pieces in 10 volumes of RIPA buffer (50 mM Tris [pH 8.0], 150 mM NaCl, 1 mM EDTA, 1.0% Triton X-100, 0.1% SDS, 0.5% sodium deoxycholate) supplemented with Complete Mini Protease Inhibitor Cocktail (Roche, reference #11836153001) at a frequency of 2.5 Hz, four times, in a benchtop bead mill homogenizer. Samples were cleared by centrifugation at $15,000 \times g$, and the supernatant was collected. Protein concentrations were determined using a bicinchoninic acid (BCA) protein assay (Pierce, catalog no. 23225) according to the manufacturer's instructions. Liver lysates (80 μg protein) were diluted in 4× NuPAGE MOPS SDS Running Buffer, NP0002 (Life Technologies, reference no. NP0007) supplemented with 5% beta-mercaptoethanol to a 20-μL final volume. Samples were denatured by heating to 95°C for 5 min and cooled on ice until gels were loaded. Proteins were resolved by SDS-PAGE on 4%–12% gradient gels (Invitrogen, reference nos. NP0322BOX and WGF1402BX10) using 3-morpholinopropane-1-sulfonic acid (MOPS) running buffer (Life Technologies, reference no. NP0002) and transferred to polyvinylidene fluoride (PVDF) membranes. Blocking was carried out for 1-hr rocking at 50 rpm on shaking platform with a 2:1 ratio of Odyssey Blocking Buffer (LI-COR Biosciences, P/N 927-40000) to PBS with 0.05% Tween 20 (PBS-T). Primary antibodies were diluted in a solution of

PBS-T supplemented with 0.1% BSA. Primary antibodies were then detected using goat anti-rabbit (680 nm; Rockland Immunochemical, RL6111440020.5) and goat anti-mouse (800 nm; Rockland Immuno-chemical, RL6111450020.5) secondary antibodies diluted in PBS-T + 0.1% BSA for 2 hr. Fluorescent imaging was performed on an Odyssey Classic Imager (LI-COR Biosciences). All western blots were performed in a similar manner, and antibody catalog numbers and dilutions are provided in Table S4.

Deep Sequencing

Genomic DNA extracted from mouse livers was amplified using locus-specific primers containing common adaptor sequences, and a second round of PCR amplification was used to add sample indexes as previously described.[45] Amplicons for all target regions were purified using magnetic beads, pooled in equimolar amounts, and sequenced using the Illumina MiSeq platform. Alignment of sequence reads to reference sequences and indel quantification were carried out as previously described.[46] All deep sequencing primers and indel analyses are provided in Tables S6–S10.

Statistics

All data are shown as the mean ± SD. Comparisons involving two groups were evaluated by a two-tailed Student's t test. For comparisons involving three or more groups, a one-way ANOVA was applied, with Tukey's post-test used to test for significant differences among groups. In all cases, significance was assigned at $p < 0.05$.

SUPPLEMENTAL INFORMATION

Supplemental Information includes six figures, ten tables, a list of plasmids used, and FASTA sequences and can be found with this article online at https://doi.org/10.1016/j.omtm.2018.11.009.

AUTHOR CONTRIBUTIONS

W.R.L., G.B., C.M.L., and A.L. conceived and designed the studies; A.L., C.M.L, A.E.H., K.E.J., M.D.G., W.L., K.S.B., A.M.D., H.D., and A.R. performed the experiments and analyzed data; A.L., W.R.L., C.M.L. and G.B. wrote the manuscript.

ACKNOWLEDGMENTS

REFERENCES

1. Ran, F.A., Cong, L., Yan, W.X., Scott, D.A., Gootenberg, J.S., Kriz, A.J., Zetsche, B., Shalem, O., Wu, X., Makarova, K.S., et al. (2015). In vivo genome editing using *Staphylococcus aureus* Cas9. Nature *520*, 186–191.

2. Yang, Y., Wang, L., Bell, P., McMenamin, D., He, Z., White, J., Yu, H., Xu, C., Morizono, H., Musunuru, K., et al. (2016). A dual AAV system enables the Cas9-mediated correction of a metabolic liver disease in newborn mice. Nat. Biotechnol. *34*, 334–338.

3. Jarrett, K.E., Lee, C.M., Yeh, Y.H., Hsu, R.H., Gupta, R., Zhang, M., Rodriguez, P.J., Lee, C.S., Gillard, B.K., Bissig, K.D., et al. (2017). Somatic genome editing with CRISPR/Cas9 generates and corrects a metabolic disease. Sci. Rep. *7*, 44624.

4. Senís, E., Fatouros, C., Große, S., Wiedtke, E., Niopek, D., Mueller, A.K., Börner, K., and Grimm, D. (2014). CRISPR/Cas9-mediated genome engineering: an adeno-associated viral (AAV) vector toolbox. Biotechnol. J. *9*, 1402–1412.

5. Ruan, G.X., Barry, E., Yu, D., Lukason, M., Cheng, S.H., and Scaria, A. (2017). CRISPR/Cas9-mediated genome editing as a therapeutic approach for Leber congenital amaurosis 10. Mol. Ther. *25*, 331–341.

6. Yu, W., Mookherjee, S., Chaitankar, V., Hiriyanna, S., Kim, J.W., Brooks, M., Ataeijannati, Y., Sun, X., Dong, L., Li, T., et al. (2017). Nrl knockdown by AAV-delivered CRISPR/Cas9 prevents retinal degeneration in mice. Nat. Commun. *8*, 14716.

7. Hung, S.S., Chrysostomou, V., Li, F., Lim, J.K., Wang, J.H., Powell, J.E., Tu, L., Daniszewski, M., Lo, C., Wong, R.C., et al. (2016). AAV-mediated CRISPR/Cas gene editing of retinal cells in vivo. Invest. Ophthalmol. Vis. Sci. *57*, 3470–3476.

8. Huang, X., Zhou, G., Wu, W., Duan, Y., Ma, G., Song, J., Xiao, R., Vandenberghe, L., Zhang, F., D'Amore, P.A., and Lei, H. (2017). Genome editing abrogates angiogenesis in vivo. Nat. Commun. *8*, 112.

9. Platt, R.J., Chen, S., Zhou, Y., Yim, M.J., Swiech, L., Kempton, H.R., Dahlman, J.E., Parnas, O., Eisenhaure, T.M., Jovanovic, M., et al. (2014). CRISPR-Cas9 knockin mice for genome editing and cancer modeling. Cell *159*, 440–455.

10. Murlidharan, G., Sakamoto, K., Rao, L., Corriher, T., Wang, D., Gao, G., Sullivan, P., and Asokan, A. (2016). CNS-restricted transduction and CRISPR/Cas9-mediated gene deletion with an engineered AAV vector. Mol. Ther. Nucleic Acids *5*, e338.

11. Guo, Y., VanDusen, N.J., Zhang, L., Gu, W., Sethi, I., Guatimosim, S., Ma, Q., Jardin, B.D., Ai, Y., Zhang, D., et al. (2017). Analysis of cardiac myocyte maturation using CASAAV, a platform for rapid dissection of cardiac myocyte gene function in vivo. Circ. Res. *120*, 1874–1888.

12. Ishizu, T., Higo, S., Masumura, Y., Kohama, Y., Shiba, M., Higo, T., Shibamoto, M., Nakagawa, A., Morimoto, S., Takashima, S., et al. (2017). Targeted genome replacement via homology-directed repair in non-dividing cardiomyocytes. Sci. Rep. *7*, 9363.

13. Tabebordbar, M., Zhu, K., Cheng, J.K.W., Chew, W.L., Widrick, J.J., Yan, W.X., Maesner, C., Wu, E.Y., Xiao, R., Ran, F.A., et al. (2016). In vivo gene editing in dystrophic mouse muscle and muscle stem cells. Science *351*, 407–411.

14. Nelson, C.E., Hakim, C.H., Ousterout, D.G., Thakore, P.I., Moreb, E.A., Castellanos Rivera, R.M., Madhavan, S., Pan, X., Ran, F.A., Yan, W.X., et al. (2016). In vivo genome editing improves muscle function in a mouse model of Duchenne muscular dystrophy. Science *351*, 403–407.

15. Long, C., Amoasii, L., Mireault, A.A., McAnally, J.R., Li, H., Sanchez-Ortiz, E., Bhattacharyya, S., Shelton, J.M., Bassel-Duby, R., and Olson, E.N. (2016). Postnatal genome editing partially restores dystrophin expression in a mouse model of muscular dystrophy. Science *351*, 400–403.

16. Davis, K.M., Pattanayak, V., Thompson, D.B., Zuris, J.A., and Liu, D.R. (2015). Small molecule-triggered Cas9 protein with improved genome-editing specificity. Nat. Chem. Biol. *11*, 316–318.

17. Zetsche, B., Volz, S.E., and Zhang, F. (2015). A split-Cas9 architecture for inducible genome editing and transcription modulation. Nat. Biotechnol. *33*, 139–142.

18. Dow, L.E., Fisher, J., O'Rourke, K.P., Muley, A., Kastenhuber, E.R., Livshits, G., Tschaharganeh, D.F., Socci, N.D., and Lowe, S.W. (2015). Inducible in vivo genome editing with CRISPR-Cas9. Nat. Biotechnol. *33*, 390–394.

19. Kleinjan, D.A., Wardrope, C., Nga Sou, S., and Rosser, S.J. (2017). Drug-tunable multidimensional synthetic gene control using inducible degron-tagged dCas9 effectors. Nat. Commun. *8*, 1191.

20. Senturk, S., Shirole, N.H., Nowak, D.G., Corbo, V., Pal, D., Vaughan, A., Tuveson, D.A., Trotman, L.C., Kinney, J.B., and Sordella, R. (2017). Rapid and tunable method to temporally control gene editing based on conditional Cas9 stabilization. Nat. Commun. *8*, 14370.

21. Maji, B., Moore, C.L., Zetsche, B., Volz, S.E., Zhang, F., Shoulders, M.D., and Choudhary, A. (2017). Multidimensional chemical control of CRISPR-Cas9. Nat. Chem. Biol. *13*, 9–11.

22. Harrington, L.B., Doxzen, K.W., Ma, E., Liu, J.J., Knott, G.J., Edraki, A., Garcia, B., Amrani, N., Chen, J.S., Cofsky, J.C., et al. (2017). A broad-spectrum inhibitor of CRISPR-Cas9. Cell *170*, 1224–1233.e15.

23. Moore, R., Spinhirne, A., Lai, M.J., Preisser, S., Li, Y., Kang, T., and Bleris, L. (2015). CRISPR-based self-cleaving mechanism for controllable gene delivery in human cells. Nucleic Acids Res. *43*, 1297–1303.

24. Merienne, N., Vachey, G., de Longprez, L., Meunier, C., Zimmer, V., Perriard, G., Canales, M., Mathias, A., Herrgott, L., Beltraminelli, T., et al. (2017). The self-inactivating KamiCas9 system for the editing of CNS disease genes. Cell Rep. *20*, 2980–2991.

25. Petris, G., Casini, A., Montagna, C., Lorenzin, F., Prandi, D., Romanel, A., Zasso, J., Conti, L., Demichelis, F., and Cereseto, A. (2017). Hit and go CAS9 delivered through a lentiviral based self-limiting circuit. Nat. Commun. *8*, 15334.

26. Cradick, T.J., Antico, C.J., and Bao, G. (2014). High-throughput cellular screening of engineered nuclease activity using the single-strand annealing assay and luciferase reporter. In Gene Correction: Methods and Protocols, F. Storici, ed. (Humana Press), pp. 339–352.

27. Cradick, T.J., Qiu, P., Lee, C.M., Fine, E.J., and Bao, G. (2014). COSMID: a web-based tool for identifying and validating CRISPR/Cas off-target sites. Mol. Ther. Nucleic Acids *3*, e214.

28. Samulski, R.J., Zhu, X., Xiao, X., Brook, J.D., Housman, D.E., Epstein, N., and Hunter, L.A. (1991). Targeted integration of adeno-associated virus (AAV) into human chromosome 19. EMBO J. *10*, 3941–3950.

29. Gil-Farina, I., Fronza, R., Kaeppel, C., Lopez-Franco, E., Ferreira, V., D'Avola, D., Benito, A., Prieto, J., Petry, H., Gonzalez-Aseguinolaza, G., and Schmidt, M. (2016). Recombinant AAV integration is not associated with hepatic genotoxicity in nonhuman primates and patients. Mol. Ther. *24*, 1100–1105.

30. Kaeppel, C., Beattie, S.G., Fronza, R., van Logtenstein, R., Salmon, F., Schmidt, S., Wolf, S., Nowrouzi, A., Glimm, H., von Kalle, C., et al. (2013). A largely random AAV integration profile after LPLD gene therapy. Nat. Med. *19*, 889–891.

31. Jarrett, K.E., Lee, C., De Giorgi, M., Hurley, A., Gillard, B.K., Doerfler, A.M., Li, A., Pownall, H.J., Bao, G., and Lagor, W.R. (2018). Somatic editing of Ldlr with adeno-associated viral-CRISPR is an efficient tool for atherosclerosis research. Arterioscler. Thromb. Vasc. Biol. *38*, 1997–2006.

32. Pan, X., Philippen, L., Lahiri, S.K., Lee, C., Park, S.H., Word, T.A., Li, N., Jarrett, K.E., Gupta, R., Reynolds, J.O., et al. (2018). In vivo Ryr2 editing corrects catecholaminergic polymorphic ventricular tachycardia. Circ. Res. *123*, 953–963.

33. Wang, L., Smith, J., Breton, C., Clark, P., Zhang, J., Ying, L., Che, Y., Lape, J., Bell, P., Calcedo, R., et al. (2018). Meganuclease targeting of PCSK9 in macaque liver leads to stable reduction in serum cholesterol. Nat. Biotechnol. *36*, 717–725.

34. Akcakaya, P., Bobbin, M.L., Guo, J.A., Malagon-Lopez, J., Clement, K., Garcia, S.P., Fellows, M.D., Porritt, M.J., Firth, M.A., Carreras, A., et al. (2018). In vivo CRISPR editing with no detectable genome-wide off-target mutations. Nature *561*, 416–419.

35. High, K.A., and Anguela, X.M. (2016). Adeno-associated viral vectors for the treatment of hemophilia. Hum. Mol. Genet. *25* (R1), R36–R41.

36. Chandler, R.J., LaFave, M.C., Varshney, G.K., Trivedi, N.S., Carrillo-Carrasco, N., Senac, J.S., Wu, W., Hoffmann, V., Elkahloun, A.G., Burgess, S.M., and Venditti, C.P. (2015). Vector design influences hepatic genotoxicity after adeno-associated virus gene therapy. J. Clin. Invest. *125*, 870–880.

37. Nault, J.C., Datta, S., Imbeaud, S., Franconi, A., Mallet, M., Couchy, G., Letouzé, E., Pilati, C., Verret, B., Blanc, J.F., et al. (2015). Recurrent AAV2-related insertional mutagenesis in human hepatocellular carcinomas. Nat. Genet. *47*, 1187–1193.

38. Büning, H., and Schmidt, M. (2015). Adeno-associated vector toxicity—to be or not to be? Mol. Ther. *23*, 1673–1675.

39. Wagner, D.L., Amini, L., Wendering, D.J., Burkhardt, L.M., Akyuz, L., Reinke, P., Volk, H.D., and Schmueck-Henneresse, M. (2018). High prevalence of *Streptococcus pyogenes* Cas9-reactive T cells within the adult human population. Nat. Med. Published online October 29, 2018. https://doi.org/10.1038/s41591-018-0204-6.

40. Chew, W.L., Tabebordbar, M., Cheng, J.K., Mali, P., Wu, E.Y., Ng, A.H., Zhu, K., Wagers, A.J., and Church, G.M. (2016). A multifunctional AAV-CRISPR-Cas9 and its host response. Nat. Methods *13*, 868–874.

41. Nathwani, A.C., Reiss, U.M., Tuddenham, E.G., Rosales, C., Chowdary, P., McIntosh, J., Della Peruta, M., Lheriteau, E., Patel, N., Raj, D., et al. (2014). Long-term safety and efficacy of factor IX gene therapy in hemophilia B. N. Engl. J. Med. *371*, 1994–2004.

42. McIntosh, J., Lenting, P.J., Rosales, C., Lee, D., Rabbanian, S., Raj, D., Patel, N., Tuddenham, E.G., Christophe, O.D., McVey, J.H., et al. (2013). Therapeutic levels of FVIII following a single peripheral vein administration of rAAV vector encoding a novel human factor VIII variant. Blood *121*, 3335–3344.

43. Lagor, W.R., Johnston, J.C., Lock, M., Vandenberghe, L.H., and Rader, D.J. (2013). Adeno-associated viruses as liver-directed gene delivery vehicles: focus on lipoprotein metabolism. Methods Mol. Biol. *1027*, 273–307.

44. Etard, C., Joshi, S., Stegmaier, J., Mikut, R., and Strähle, U. (2017). Tracking of indels by DEcomposition is a simple and effective method to assess efficiency of guide RNAs in zebrafish. Zebrafish *14*, 586–588.

45. Lin, Y., Cradick, T.J., Brown, M.T., Deshmukh, H., Ranjan, P., Sarode, N., Wile, B.M., Vertino, P.M., Stewart, F.J., and Bao, G. (2014). CRISPR/Cas9 systems have off-target activity with insertions or deletions between target DNA and guide RNA sequences. Nucleic Acids Res. *42*, 7473–7485.

46. Lee, C.M., Cradick, T.J., and Bao, G. (2016). The *Neisseria meningitidis* CRISPR-Cas9 system enables specific genome editing in mammalian cells. Mol. Ther. *24*, 645–654.